Proc. of the European Safety and Reliability Conference (ESREL 2026)
Edited by José C. Matos, Paulo B. Lourenço, Michael Beer, Daniel Oliveira, Edoardo Patelli, Hélder S. Sousa, Rui A. Silva and Monica Santamaria
 Published by Research Publishing, Singapore.
doi: 10.3850/ESREL2026061419_esrel26-p29111-cd

Risk Assessment and Safety Barrier Importance Measure for Multi-State Electromechanical Systems Considering Competing Failure Mechanisms

Ximing Luo

School of Reliability and Systems Engineering, Beihang University, China. E-mail: luoximing123456@buaa.edu.cn

Jian Jiao

School of Reliability and Systems Engineering, Beihang University, China. E-mail: jiaojian@buaa.edu.cn

Yongfeng Jing

School of Reliability and Systems Engineering, Beihang University, China. E-mail: yongfengjing@buaa.edu.cn

Yuan Yuan

School of Reliability and Systems Engineering, Beihang University, China. E-mail: yuan_yuan@buaa.edu.cn

Electromechanical systems comprise multiple interconnected components that are susceptible to progressive degradation and competing failure modes driven by various underlying physical mechanisms during prolonged operation. Most existing risk assessment studies for such systems focus on binary-state assumptions and single failure mode scenarios, overlooking the importance of multi-state degradation characterization and the competing interactions among these modes. This paper proposes a risk assessment and safety barrier importance evaluation method for multi-state electromechanical systems that quantifies system risk and barrier importance by incorporating competing failure modes and multi-state degradation processes. A multi-state Bow-tie modeling framework based on semi-Markov process theory is first established to capture the evolutionary behavior of system components under dynamically varying degradation conditions through state transition mechanisms. A competing failure semi-Markov model (CF-SMM) is then constructed by integrating these multiple failure modes, thereby overcoming the limitations of conventional exponential distribution assumptions and single failure mode assumptions. Subsequently, a safety barrier importance measure (SBIM) is developed by fusing risk sensitivity, structural relevance, and state degradation degree to maximize barrier discrimination capability. Finally, the proposed method is validated through a case study of a five-axis machining center as a representative electromechanical system. The results demonstrate that the monotonicity index of the SBIM method reaches 1.00 at t = 8760 h, representing improvements of 8.7% and 13.6% over the Birnbaum importance and Fussell-Vesely importance measures, respectively. The proposed method enhances both risk assessment accuracy and barrier importance discrimination for electromechanical systems, providing methodological support for maintenance resource optimization and operational safety assurance in dynamic degradation environments.

Keywords: Electromechanical systems, competing failures, semi-Markov processes, bow-tie models, safety-barrier importance.

1. Introduction

Electromechanical systems serve as core equipment in modern manufacturing and play critical roles in intelligent manufacturing scenarios such as aerospace, automotive manufacturing, and precision machining. Despite their widespread application, operational safety remains a persistent concern due to frequent equipment failures triggered by component degradation. System failures fundamentally originate from the progressive degradation of component performance during prolonged operation, including accelerated bearing wear (Zhang et al. 2025a), electrical insulation aging (Choudhary et al. 2025), and sensor accuracy deterioration (Wang et al. 2025). Moreover, a single component is often simultaneously subjected to the competitive effects of multiple failure modes, where the failure mode that triggers first determines the actual degradation path (Huang and Askin 2003; Wu et al. 2024).

The Bow-tie model, as an integrated risk analysis framework combining fault tree analysis and event tree analysis, has been widely applied in risk assessment (Yang et al. 2025; Xu et al.

2026). However, conventional Bow-tie models treat components as binary-state entities, making it difficult to characterize progressive degradation dynamics. While Markov processes are widely adopted for multi-state systems, their exponential distribution assumption fails to accurately describe degradation processes with increasing failure rates, such as mechanical wear and fatigue. Therefore, Semi-Markov Processes (SMP), which have long been established as a rigorous mathematical framework for reliability analysis involving arbitrary sojourn times (Limnios and Oprisan 2001), are required to capture these realistic degradation behaviors. Furthermore, a single component in electromechanical systems is rarely subjected to a single stressor; instead, it faces the concurrent presence of multiple failure modes. The failure mode that reaches its critical threshold first determines the actual state transition behavior. Most existing studies overlook this competing failure phenomenon, leading to biased risk estimations. Regarding importance measures, current methods focus on a single dimension and fail to comprehensively account for the structural position, risk sensitivity, and degradation state of barriers (Zhang et al. 2025b).

To address these gaps, this paper proposes a competing failure semi-Markov model (CF-SMM) and a safety barrier importance measure (SBIM) methodology. The main contributions include: (1) a multi-state Bow-tie modeling approach employing SMP framework to capture degradation evolution; (2) a CF-SMM integrating concurrent effects of multiple failure modes for dynamic risk assessment; (3) an SBIM metric synthesizing risk sensitivity, structural relevance, and state degradation severity for enhanced barrier discrimination.

2. Multi-state Electromechanical System Competing Failure Modeling Based on the Bow-tie Model

Components of electromechanical systems inevitably undergo performance degradation during prolonged operation, causing system risk levels to evolve continuously. Conventional Bow-tie models treat system components as binary-state entities, making it difficult to characterize progressive degradation and its dynamic impact on risk. Furthermore, system components typically face competitive effects of multiple failure modes — the same component may experience competing failures caused by different physical mechanisms, with the failure mode that occurs first determining the actual degradation path. This section constructs a modeling approach that accounts for multi-state degradation and competing failure within the Bow-tie model framework, based on semi-Markov process (SMP) theory.

2.1. *System architecture modeling based on the Bow-tie model*

To capture the continuous evolution of accidents from initial threat incubation to ultimate damage, the Bow-tie model is adopted. Furthermore, since traditional binary-state models fail to capture the physics of progressive wear, we extend this model into a multi-state framework to accurately map component degradation to dynamic system risk. Building upon the foundational framework proposed by de Dianous and Fiévez (2006), our proposed multi-state Bow-tie model adopts a bowtie-shaped topology with the electromechanical system accident as the top event. The left side employs fault tree analysis (FTA) to examine the propagation paths from threat events to the top event, while the right side uses event tree analysis (ETA) to examine the evolution paths from the top event to consequence events. Comprising four core components, it is represented as a four-tuple in Eq.(1).

$$BT = (T, TE, C, B) \tag{1}$$

In Eq.(1), T, TE, C, and $B = B^P \cup B^M$ represent sets of threats, top event, consequences, and barriers (preventive B^P and mitigative B^M), respectively.The structure function for threat event T_j triggering the top event is defined in Eq.(2).

$$\phi_j^{FT}(x^T, x^P) = x_j^T \cdot \prod_{i:a_{ji}^{TP}=1} x_i^P \tag{2}$$

Where $x_j^T \in \{0,1\}$ is the state indicator for threat event T_j, $x_i^P \in \{0,1\}$ is the failure state indicator for preventive barrier B_i^P, and a_{ji}^{TP} is the element of the threat–preventive barrier association matrix. The structure function for the top event occurrence is given by Eq.(3).

$$\phi^{TE}(x^T, x^P) = 1 - \prod_{j=1}^{m}[1 - \phi_j^{FT}(x^T, x^P)] \quad (3)$$

For any Bow-tie model component $E \in T \cup B \cup C$, its discrete state space $S_E = \{0,1,2,\ldots,K_E\}$ is partitioned by a critical state k_E^{cr} into normal states $S_E^N = \{0,1,\ldots,k_E^{cr}-1\}$ and failed states $S_E^F = \{k_E^{cr}, k_E^{cr}+1,\ldots,K_E\}$, where K_E is the maximum degradation level.

Binary association matrices $A^{TP} = [a_{ji}^{TP}]_{m\times p}$ and $A^{MC} = [a_{il}^{MC}]_{q\times n}$ map the topological interrelationships, where $a_{ji}^{TP} = 1$ ($a_{il}^{MC} = 1$) indicates barrier B^{pP} (B^{pM}) is deployed on the propagation path of T_j to TE (TE to C_l).

2.2. *Multi-state electromechanical system degradation process modeling*

The degradation process of each component is influenced by physical mechanisms, operational environments, and loading conditions. Threat events can be classified based on degradation mechanisms: mechanical performance degradation threats typically arise from transmission component wear and exhibit progressive accumulation with increasing failure rates; electrical performance degradation threats can be triggered by a variety of underlying mechanisms (e.g., contact oxidation, thermal aging of insulation). Consequently, they are modeled using various distributions depending on the specific physics of failure (Montanari and Simoni, 1993); for instance, multi-physics coupling effects such as insulation aging are often characterized by a lognormal distribution; control performance degradation threats arise from factors like sensor drift and may manifest as gradual or abrupt modes.

For threat event T_j, its state space is $S_{T_j} = \{0,1,\ldots,K_{T_j}\}$. For mechanically wear-dominated threats, the Weibull distribution describes the sojourn time as in Eq.(4).

$$f_i^{T_j}(t) = \frac{\beta_{ij}^T}{\alpha_{ij}^T}\left(\frac{t}{\alpha_{ij}^T}\right)^{\beta_{ij}^T-1} exp\left[-\left(\frac{t}{\alpha_{ij}^T}\right)^{\beta_{ij}^T}\right] \quad (4)$$

For electrically aging-dominated threats, the lognormal distribution is adopted as in Eq.(5).

$$f_i^{T_j}(t) = \frac{1}{t\sigma_{ij}^T\sqrt{2\pi}} exp\left[-\frac{(ln\ t-\mu_{ij}^T)^2}{2(\sigma_{ij}^T)^2}\right] \quad (5)$$

For safety barriers, both preventive and mitigative barriers share similar degradation mechanisms. For barriers dominated by electronic components, the Gamma distribution is employed as in Eq.(6).

$$f_k^{B_i^P}(t) = \frac{(\lambda_k^{B_i})^{n_k^{B_i}}}{\Gamma(n_k^{B_i})} t^{n_k^{B_i}-1} exp\left(-\lambda_k^{B_i} t\right) \quad (6)$$

The parameters ($\alpha_{ij}^T, \beta_{ij}^T$) for Weibull, ($\mu_{ij}^T, \sigma_{ij}^T$) for Lognormal, and ($n_k^{B_i}, \lambda_k^{B_i}$) for Gamma distributions are determined by the specific failure physics of the components.

Mitigative barriers $B_l^M (l = 1,2,q)$, share physical similarities with preventive barriers and thus adopt the same modeling framework, state space $S_{B_l^M}$, and mechanism-matching distributions (Weibull, Gamma, or Lognormal) for their sojourn time $H_k^{B_l^M}$.

For consequence events, the state space $S_{C_l} = \{0,1,\ldots,K_{C_l}\}$ represents severity levels. Given the irreversibility of consequences, state transitions are modeled as unidirectional increasing processes. The transition probability matrix $P^{C_l} = [p_{ij}^{C_l}]$ is upper triangular, satisfying $p_{ij}^{C_l} = 0$ for all $i > j$. This constraint ensures that consequence severity can only be maintained or worsened, consistent with the actual physical process.

2.3. *Competing failure semi-Markov model construction*

Components of electromechanical systems typically face concurrent effects of multiple failure modes. Competing failure refers to the simultaneous exposure of a single component to failure threats caused by different physical mechanisms, where the failure mode that occurs first determines the actual state transition.

2.3.1. *Semi-Markov process framework*

Mechanical and electrical degradation involves cumulative fatigue and aging, violating the constant failure rate assumption of standard Markov models. Thus, the SMP is employed, as it allows arbitrary sojourn time distributions (e.g., Weibull, Lognormal) to match actual physical wear-out mechanisms.For component $E \in \{T \cup B \cup C\}$, the semi-Markov kernel function is given in Eq.(7).

$$Q_{ij}^{E}(t) = P(X_{n+1}^{E} = j, \tau_{n+1}^{E} - \tau_{n}^{E} \le t \mid X_{n}^{E} = i) = p_{ij}^{E} F_{i}^{E}(t) \quad (7)$$

Where p_{ij}^{E} is the transition probability of the embedded Markov chain, and $F_i^E(t)$ is the cumulative distribution function of the sojourn time. The transient probability $\pi_j^E(t)$ satisfies the Markov renewal equation as in Eq.(8).

$$\pi_j^E(t) = \delta_j^E(0)\bar{F}_j^E(t) + \sum_{i \in S_E, i \neq j} \int_0^t \pi_i^E(t-\tau) p_{ij}^E f_i^E(\tau) d\tau \quad (8)$$

The Markov renewal equation system is numerically solved using a discrete-time approximation. The continuous time interval [0, T] is discretized into N equally spaced time points with time step $\Delta t = T/N$ and discrete time points $t_k = k\Delta t (k = 0,1,N)$. Under the discrete-time framework, the Markov renewal equation transforms into a recursive form as in Eq.(9).

$$\pi_j^E(t_{k+1}) = \delta_j^E(0)\bar{F}_j^E(t_{k+1}) + \sum_{i \in S_E, i \neq j} \sum_{l=0}^{k} \pi_i^E(t_{k-l}) p_{ij}^E f_i^E(t_l) \quad (9)$$

In Eq.(8), $\delta_j^E(0), \bar{F}_j^E(t)$ and $f_i^E(t)$ denote the initial state indicator, survival function, and probability density function, respectively. For numerical stability, Eq.(9) is solved recursively with $\Delta t \ll \min_i \{E[H_i^E]\}$.

2.3.2. *Competing failure modeling*

Let safety barrier B in state k face a set of M failure modes $\{FM_1, FM_2, \ldots, FM_M\}$. The time for each failure mode FM_r acting independently to cause state transition is a random variable $H_k^{(r)}$ with survival function $F_k^{(r)}(t)$. Under the competing failure mechanism, the actual state transition time is determined by the earliest occurring failure mode: $H_k = min\{H_k^{(1)}, H_k^{(2)}, H_k^{(M)}\}$.

Assuming mutual independence among failure modes, the survival function of the equivalent sojourn time H_k is the product of the survival functions of individual failure modes (see Eq.(10)).

$$\bar{F}_k(t) = P(H_k > t) = \prod_{r=1}^{M} P(H_k^{(r)} > t) = \prod_{r=1}^{M} \bar{F}_k^{(r)}(t) \quad (10)$$

The corresponding probability density function is derived by differentiating Eq.(10), yielding Eq.(11).

$$f_k(t) = \frac{dF_k(t)}{dt} = \sum_{r=1}^{M} f_k^{(r)}(t) \prod_{l \neq r} \bar{F}_k^{(l)}(t) \quad (11)$$

The cause-specific hazard rate function for failure mode FM_r is defined as $h_k^{(r)}(t) = \frac{f_k^{(r)}(t)}{\bar{F}_k^{(r)}(t)}$, characterizing the instantaneous probability of failure caused by failure mode r at time t. Given that failure has occurred at time t, the time-varying transition probability from state k to state j is given by Eq.(12).

$$p_{kj}(t) = \frac{\sum_{r=1}^{M} \gamma_{kj}^{(r)} h_k^{(r)}(t)}{\sum_{r=1}^{M} h_k^{(r)}(t)} \quad (12)$$

Where $\gamma_{kj}^{(r)}$ is the indicator function for failure mode FM_r causing transition from state k to state j. The semi-Markov kernel function under competing failure is :formulated in Eq.(13).

$$Q_{kj}(t) = \int_0^t p_{kj}(\tau) f_k(\tau) d\tau = \sum_{r=1}^{M} \gamma_{kj}^{(r)} \int_0^t f_k^{(r)}(\tau) \prod_{l \neq r} \bar{F}_k^{(l)}(\tau) d\tau \quad (13)$$

The same modeling approach applies to threat events. Based on this CF-SMM framework, the joint system state space can be defined as $S(t) = (s^T(t), s^P(t), s^M(t), s^C(t))$, providing the foundation for subsequent dynamic risk quantification.

3. Risk and Safety Barrier Importance Assessment for Multi-state Electromechanical Systems Based on CF-SMM

Building upon the CF-SMM established in Section 2, this section constructs a dynamic risk quantification method and proposes a safety barrier importance measure (SBIM) that comprehensively considers risk sensitivity, structural relevance, and state degradation severity.

3.1. *Risk quantification based on CF-SMM*

System risk originates from the activation of threat events, the failure of safety barriers, and the manifestation of consequences.

For threat event T_j, its activation probability at time t is defined in Eq.(14).

$$P_{act}^{T_j}(t) = P\left(s_j^T(t) \in S_{T_j}^A\right) = \sum_{k=1}^{K_{T_j}} \pi_k^{T_j}(t) = 1 - \pi_0^{T_j}(t) \quad (14)$$

For preventive barrier B_i^P, its failure probability at time t is calculated using Eq.(15).

$$P_F^{B_i^P}(t) = P\left(s_i^P(t) \in S_{B_i^P}^F\right) = \sum_{k=k_i^{cr}}^{K_{B_i^P}} \pi_k^{B_i^P}(t) \quad (15)$$

The probability of threat T_j triggering the top event at time t is given by Eq.(16).

$$P(TE|T_j,t) = P_{act}^{T_j}(t) \cdot \prod_{i:a_{ji}^{TP}=1} P_F^{B_i^P}(t) \quad (16)$$

The top event occurrence probability at time t, considering contributions from all threat events, is computed using the inclusion–exclusion principle, as expressed in Eq.(17).

$$P(TE,t) = 1 - \prod_{j=1}^{m} [1 - P(TE|T_j,t)] \quad (17)$$

Following the top event, the occurrence probability of consequence C_l depends on mitigative barriers, as shown in Eq.(18).

$$P(C_l|TE,t) = \prod_{i:a_{li}^{MC}=1} P_F^{B_i^M}(t) \quad (18)$$

The severity S_l of consequence event C_l comprises direct losses C_l^D and indirect losses C_l^I: $S_l = C_l^D + C_l^I$. The system risk index at time t is then obtained from Eq.(19).

$$RI(t) = P(TE,t) \cdot \sum_{l=1}^{n} P(C_l|TE,t) \cdot S_l \quad (19)$$

3.2. *Safety barrier importance measure definition and assessment*

Multiple factors jointly influence how a safety barrier affects system risk: its topological position in the Bow-tie model determines its structural importance, the marginal impact of barrier failure probability changes on system risk determines its risk sensitivity, and its current degradation state determines its urgency. Based on this analysis, the SBIM is decomposed into a composite metric of three dimensions, as defined in Eq.(20).

$$I_B^{SBIM}(t) = I_B^{RS}(t) \cdot I_B^{SC} \cdot I_B^{SD}(t) \quad (20)$$

Where $I_B^{RS}(t)$, I_B^{SC}, $I_B^{SD}(t)$ represent risk sensitivity, structural relevance, and state degradation severity, respectively. This multiplicative form ensures that all three dimensions jointly contribute to the importance calculation, where a significant change in any dimension produces a noticeable impact on the SBIM.

3.2.1. *Risk sensitivity*

Risk sensitivity is defined as the partial derivative of the system risk index with respect to barrier failure probability, as given in Eq.(21).

$$I_B^{RS}(t) = \frac{\partial RI(t)}{\partial P_F^B(t)} \quad (21)$$

For preventive barrier B_i^P, the risk sensitivity can be obtained through analytical differentiation, as presented in Eq.(22).

$$I_{B_i^P}^{RS}(t) = \sum_{j:a_{ji}^{TP}=1} P_{act}^{T_j}(t) \cdot \prod_{i':a_{ji'}^{TP}=1, i' \neq i} P_F^{B_{i'}^P}(t) \cdot \prod_{j' \neq j} [1 - P(TE|T_{j'},t)] \cdot \sum_{l=1}^{n} S_l \cdot \prod_{i'':a_{li''}^{MC}=1} P_F^{B_{i''}^M}(t) \quad (22)$$

For mitigative barrier B_l^M, the risk sensitivity is similarly derived, as shown in Eq.(23).

$$I_{B_l^M}^{RS}(t) = P(TE,t) \cdot \sum_{l':a_{ll'}^{MC}=1} S_{l'} \cdot \prod_{i:a_{ll'}^{MC}=1, i\neq l} P_F^{B_i^M}(t) \quad (23)$$

The time-varying nature of risk sensitivity stems from the evolution of threat activation probabilities and other barriers' failure probabilities.

3.2.2. *Structural relevance*

Structural relevance reflects the barrier's topological importance, determined by the number and severity of associated threat or consequence events.

For preventive barrier B_i^P, the structural relevance is defined in Eq.(24).

$$I_{B_i^P}^{SC} = \frac{\sum_{j:a_{ij}^{TP}=1} \bar{S}_j}{\sum_{j=1}^{m} \bar{S}_j} \quad (24)$$

Where $\bar{S}_j$ is the average consequence severity that may result from threat T_j triggering the top event.

For mitigative barrier B_l^M, the structural relevance is defined in Eq.(25).

$$I_{B_l^M}^{SC} = \frac{\sum_{l':a_{ll'}^{MC}=1} S_{l'}}{\sum_{l'=1}^{n} S_{l'}} \quad (25)$$

The design of structural relevance ensures that barriers in different topological positions of the Bow-tie model receive different baseline importance values.

3.2.3. *State degradation severity*

State degradation severity reflects the current health status using the expected degradation level, as formulated in Eq.(26).

$$I_B^{SD}(t) = \frac{\sum_{k=0}^{K_B} k \cdot \pi_k^B(t)}{K_B} + \epsilon \quad (26)$$

Where $\pi_k^B(t)$ is the probability of barrier B being in state k at time t, K_B is the maximum degradation state, and ϵ (e.g., $\epsilon = 0.1$) prevents a zero value for perfectly intact barriers.

4. Case Study

A five-axis machining center is selected as the case study, representing a typical complex electromechanical system integrating mechanical, electrical, hydraulic, and control subsystems. Based on failure mode and effects analysis (FMEA) and field failure records, the Bow-tie model is constructed with 15 threat events, seven preventive barriers, three mitigative barriers, and three consequence events. The top event TE is defined as "critical function failure of the machining center." Consequence events include C_1 (equipment damage, S_1 = 250,000 Chinese yuan (CNY)), C_2 (product quality defects, S_2 = 150,000 CNY), and C_3 (personnel safety accidents, S_3 = 800,000 CNY).

All components adopt a four-state partition with state space S = {0,1,2,3}. Competing failure modes for threat events and safety barriers are identified based on their failure mechanisms, with distribution parameters estimated from equipment reliability data. Distribution selection follows mechanism-matching principles: mechanically wear-dominated failures adopt the Weibull distribution, electrically aging-dominated failures adopt the lognormal distribution, and random shock-dominated failures adopt the exponential distribution.

Table 1 presents a representative set of components covering mechanical, electrical, and control domains, detailing their competing failure parameters and topological associations.

4.1. *Computational results*

The system risk index $RI(t)$ under different scenarios is computed using Eq.(19), with evolution curves shown in Fig. 1. $RI(t)$ remains low during early operation (0 – 2000 h), accelerates during mid-operation with $RI(t)$ = 0.43 at t = 4000 h, and reaches 9.50 at t = 8760 h. This demonstrates that preventive barriers dominate risk control during early operation, while mitigative barriers become more significant during late operation.

Table 1. Representative set of components, competing failure modes, and parameters

ID	Component Name	Topological Associations	Failure Modes	Distribution	Parameters
T_1	Spindle bearing functional degradation	B_1^P, B_4^P	FM_1: Abrasive wear	Weibull	α=5000h, β=2.2
			FM_2: Fatigue spalling	Weibull	α=6500h, β=2.5
T_2	Spindle motor performance degradation	B_1^P, B_4^P	FM_1: Winding insulation aging	Lognormal	μ=8.5, σ=0.4
			FM_2: Bearing wear	Weibull	α=7000h, β=2.0
T_{13}	Main contactor functional degradation	B_4^P, B_5^P	FM_1: Contact oxidation	Gamma	n=2, λ=0.0007/h
			FM_2: Arc erosion	Weibull	α=4500h, β=1.7
B_1^P	Spindle vibration sensor	T_1, T_2, T_3, T_8	FM_1: Piezo crystal degradation	Weibull	α=7000h, β=2.2
			FM_2: Circuit aging	Lognormal	μ=8.4, σ=0.4
B_1^M	Emergency stop button	C_1, C_2, C_3	FM_1: Reset spring fatigue	Weibull	α=10000h, β=2.5
			FM_2: Contact degradation	Gamma	n=3, λ=0.0003/h

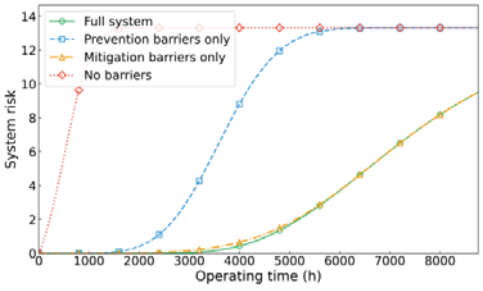

Fig. 1. System risk evolution under different scenarios

The SBIM evolution curves for all barriers are obtained using Eq.(20), as shown in Fig. 2 and Fig. 3. Among preventive barriers, B_2^{P} (encoder verification module) achieves the highest SBIM value of 0.746 at t = 8760 h due to its association with multiple threat events. Among mitigative barriers, B_2^{M} reaches 0.962 at t = 8760 h. The ratio between the highest and lowest SBIM values reaches 3.5 times at t = 8760 h, demonstrating significant discrimination capability.

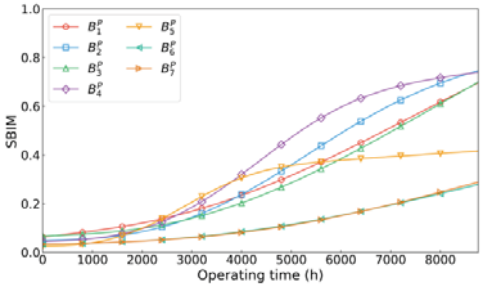

Fig. 2. Preventive barrier importance measure evolution

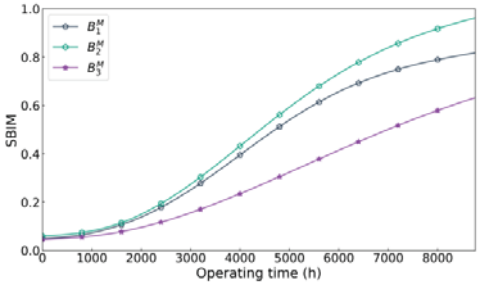

Fig. 3. Mitigative barrier importance measure evolution

4.2. *Performance comparison*

The monotonicity index $M(\alpha)$ is introduced to evaluate the discrimination capability of different importance measures , as defined in Eq. (27).

$$M(\alpha) = \left(1 - \frac{1}{M(M-1)} \sum_{r \in \alpha} n_r \left(n_r - 1\right)\right)^2 \quad (27)$$

Where α is the importance ranking result vector, M is the total number of barriers, and n_r is the number of barriers with importance value r. $M(\alpha) \in [0,1]$, where $M(\alpha) = 1$ indicates that all barrier importance values are distinguishable, and $M(\alpha) = 0$ indicates that all barriers have identical importance values and cannot be discriminated.

The Birnbaum importance (BI) and Fussell–Vesely importance (FV) are selected as benchmark methods for comparison with the proposed SBIM method. The monotonicity index results at different time instants are presented in Table 2.

Table 2. Monotonicity index comparison of different importance measures at various time instants

Time (h)	BI	FV	SBIM
2000	0.82	0.78	0.95
4000	0.86	0.82	0.94
6000	0.9	0.86	0.99
8760	0.92	0.88	1

The proposed SBIM method achieves monotonicity index of 1.00 at t = 8760 h , representing improvements of 8.7% over BI and 13.6% over FV. These results demonstrate that SBIM possesses stronger barrier discrimination capability through its synthesis of risk sensitivity, structural relevance, and state degradation severity, providing more reliable decision support for differentiated maintenance resource allocation.

5. Conclusion

This paper investigated competing failure mechanisms and multi-state degradation effects on risk assessment and barrier importance evaluation for electromechanical systems. A CF-SMM integrating multiple failure modes was established, and an SBIM methodology synthesizing risk sensitivity, structural relevance, and state degradation severity was proposed.

Validation through a five-axis machining center case study demonstrates that the SBIM method achieves a monotonicity index of 1.00 at t = 8760 h—an improvement of 8.7% over Birnbaum importance and 13.6% over Fussell–Vesely importance. Preventive barriers dominate risk control during early operation, while mitigative barriers become more significant later. The methodology provides practical support for maintenance resource optimization and operational safety assurance. Future work may incorporate component dependency modeling and conduct comparative studies across multiple equipment types.

References

Choudhary, M., I. Kiitam, and I. Palu (2025). Electrical aging and lifetime study of Nomex insulation influenced by partial discharges. Electric Power Systems Research 249, 112000.

de Dianous, V., and C. Fiévez (2006). ARAMIS project: A more explicit demonstration of risk severity and risk control through the use of bow-tie diagrams and the evaluation of safety barrier performance. Journal of Hazardous Materials 130(3), 220-233.

Huang, H. Z., and R. G. Askin (2003). Reliability analysis of electronic devices with multiple competing failure modes. Quality and Reliability Engineering International 19(3), 241-254.

Limnios, N., and G. Oprisan (2001). Semi-Markov Processes and Reliability. Boston: Birkhäuser.

Montanari, G. C., & Simoni, L. (1993). Aging phenomenology and modeling. IEEE Transactions on Electrical Insulation, 28(5), 755-776.

Wang, W., Z. Wang, Z. Cai, et al. (2025). Robust uncertainty quantification for online remaining useful life prediction with randomly missing and partially faulty sensor data. Reliability Engineering & System Safety 262, 111177.

Wu, B., X. Zhang, H. Shi, et al. (2024). Failure mode division and remaining useful life prognostics of multi-indicator systems with multi-fault. Reliability Engineering & System Safety 244, 109961.

Xu, Y., P. Peng, C. Claramunt, et al. (2026). Resilience of the global maritime LNG network: From static Bow-tie to dynamic SIR modeling. Reliability Engineering & System Safety 265, 111605.

Yang, D., X. Huang, B. Xie, et al. (2025). Multidimensional causation chain analysis of marine oil spill accidents: Based on grounded theory and Bow-tie model. Ocean Engineering 341, 122824.

Zhang, K., M. Wang, Y. Zhang, et al. (2025a). Wear performance evaluation of journal bearings in wind turbine gearbox. International Journal of Mechanical Sciences 297 – 298, 110346.

Zhang, C., J. Qiao, S. Wang, et al. (2025b). Importance measures based on system performance loss for multi-state phased-mission systems. Reliability Engineering & System Safety 256, 110776.